Automedica, 2001, Vol. 20, pp. 297–312
Reprints available directly from the publisher
Photocopying permitted by license only

ON DNA MODELLING: INTERACTION OF A DOUBLE HELICOIDAL STRUCTURE WITH VISCOUS BIO-FLUID

C. W. LIM[a] and JIAN-JUN SHU[b,*]

[a]*Department of Building and Construction, City University of Hong Kong, Tat Chee Avenue, Kowloon, Hong Kong;* [b]*School of Mechanical and Production Engineering, Nanyang Technological University, 50 Nanyang Avenue, Singapore 639798*

(Received 20 September 2001; In final form 10 October 2001)

The paper aims at extending, utilising and generalising research in nonlinear dynamics of (i) spiral/helicoidal structures, and (ii) viscous, low speed fluid to biomechanical DNA fluid-structure interaction. Employing a nonlinear helicoidal model, the energy stored in a distorted Watson–Crick DNA model subjected to viscous, low speed organic fluid loading is formulated. Numerical solutions based on the variational principle are presented for a linearized flow field as examples. Significant dynamical responses such as deformation components and resultants are discussed. A proposal for matching of DNA sequential characteristics with respect to the nonlinear dynamical responses is outlined in order to reveal information regarding DNA sequencing by means of a fluid-structure dynamical approach.

Keywords: DNA modelling; Double helicoidal structure; Strain energy; Variational principle; Viscous bio-fluid; Work

1 INTRODUCTION

Although Deoxyribonucleic acid (DNA) was first identified as a kind of acid in a cell nucleus over 100 years ago, the way by which two polynucleotide chains are held together in a helical manner with A–T and G–C pairing bases was only discovered by James Watson and Francis Crick [1] in 1953. This model has been widely discussed and several alternative models have

* Corresponding author. Fax: 65 6791 1859; E-mail: mjjshu@ntu.edu.sg

also been proposed [2]. In general, DNA is constructed from two inconceivably long and heavily supercoiled helical polymers, commonly referred to as the Watson–Crick double helix model. It is known as one of the most interesting and mysterious biological molecules having an ability to conserve, replicate and transfer genetic information. It has been discovered as an acid in a cell nucleus for more than 100 years, and its biological aspects have been established to a certain advanced level today. However, the understanding of nonlinear physical properties of DNA is still far from sufficient for accurate prediction of its dynamical responses. The knowledge of molecular biomechanics is important because almost all aspects of life are engineered at that level. As Francis Crick mentioned "*All approaches at a higher level are suspect until confirmed at the molecular level*" [3].

There exists intensive research in biological and chemical DNA analyses [4]. A comprehensive review of the essential works is out of scope, and will not be presented. Three events stimulated the appearance and rapid development of nonlinear DNA physics [5, 6]. The first was the success of nonlinear mathematics and its application to many physical phenomena. The second was the emergence of new results in the dynamics of biopolymers, which has led to an understanding of the important role of dynamics in the biological functioning of biopolymers. The third event was the publications of Davydov [5] where, for the first time, the achievements of nonlinear mathematics were applied to biology and the occurrence of solitons in biopolymers was hypothesized. One of the earliest research works on the nonlinear physics of DNA was attributed to Englander *et al.* [6] who introduced the nonlinear conformational excitations and presented the first nonlinear Hamiltonian of DNA, which gave a powerful impulse for theoretical investigations. A number of investigators [2] improved the Hamiltonian model and its dynamical parameters, by investigating corresponding nonlinear differential equations and their soliton-like solutions with consideration of DNA solitons and calculation of corresponding correlation functions. The results [5, 6] formed a theoretical basis for the nonlinear physics of DNA.

DNA is not motionless. It is in a constantly wriggling dynamic state in a medium of bioorganic fluid in the nucleus of a cell. DNA can be modelled as a double twisted helicoidal structure [2, 4] constantly interacting with surrounding viscous, organic fluid. Almost all existing DNA analyses assume a very coarse dynamical model. Among them are the rod-like models, the double rod-like models and the nonlinear higher-level models [2]. Complexity was introduced by adding the effects of environment, inhomogeneity,

helicity and nonlinear excitations [2]. The rod-like models disregard DNA helical effects, and assume a coiled double helix as a single rod. They are only good if we are interested in examining the global responses of DNA at a coarser level. As the Watson–Crick model features a double helix, the rod-like models are too crude to study the interior twisting, deformation and distribution of energy.

For the reasons above, we present a new innovative approach to investigate the nonlinear dynamics of DNA in this paper. The DNA molecule is modelled, from a physical viewpoint, as an interactive fluid-structure complex dynamical system, having a two-dimensional helicoidal structure [7–12] immersed in viscous bio-fluids. The model proposed here is more refined than the elastic rod-like models such as that of Barkley ad Zimm [13] and Allison and Shurr [14]. It can be developed from expertise in the modelling of helicoidal structures, because the model can be formed by limiting the width of a drill [11, 12]. In other words, a helix is a special subset of a drill, and therefore the dynamic responses of a double helix can be investigated from the knowledge of dynamics of drilling structures. The viscous bio-fluids surrounding DNA are considered as Low–Reynolds number fluids, and fundamental solutions can be obtained by solving the unsteady Stokes flow equation [15, 16]. The fluid-structure system can be characterised by specific distributions of internal forces and energy, and internal motions including deformation, bending and twisting could be determined from the unsteady viscous flow loadings. These dynamical characteristics and responses will assist in the classification of various types of DNA.

2 ENGINEERING DNA MODEL

The geometry of a helix or a helicoil with length a, radius R, width b and projected angle θ_0 (at a) are shown in Figures 1 and 2. When the condition $b < R \ll a$, where b is about an order smaller than R [2] is imposed, a helicoil (Fig. 3) is obtained. Although not shown in this figure, the thickness h of the helicoil considered *may not necessarily be a constant.* It could vary such that the cross section is *round* or *any other shape*, so that the helicoil model is more realistic. The Watson–Crick double helix DNA model can be constructed as a combination of such two parallel helicoils with internal bondings as shown in Figure 4(a), which can be used to model a DNA molecule as shown in Figure 4(b).

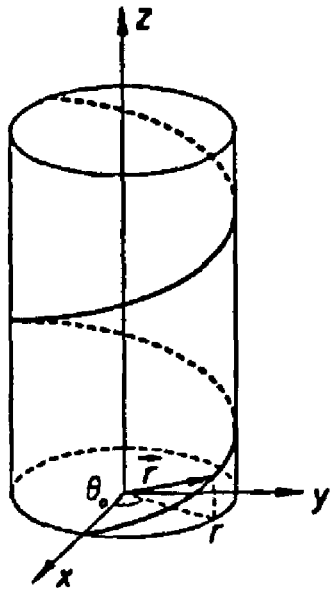

FIGURE 1 Geometry of a helix.

A curvilinear coordinate system, perpendicular and tangential to the helix and lying in the osculating plane $(\vec{\mathbf{r}}, \partial\vec{\mathbf{r}}/\partial\theta)$, is adopted. With the binormal vector to the helix $\vec{\mathbf{b}}$, it forms an orthogonal coordinate system $(\vec{\mathbf{r}}, \partial\vec{\mathbf{r}}/\partial\theta, \vec{\mathbf{b}})$, and its transformation with respect to the Cartesian system $(\vec{\mathbf{i}}, \vec{\mathbf{j}}, \vec{\mathbf{k}})$ is

$$\vec{\mathbf{r}} = r(\vec{\mathbf{i}}\cos\theta + \vec{\mathbf{j}}\sin\theta) + \frac{\theta}{\varphi}\vec{\mathbf{k}} \tag{1}$$

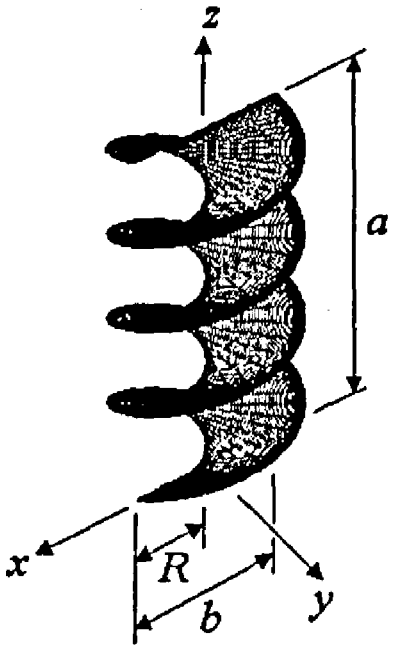

FIGURE 2 Geometry of a helicoidal structures.

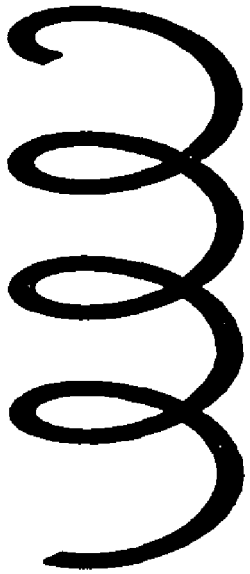

FIGURE 3 Geometry of a helicoil.

where $\varphi = \theta_0/a$ is the rate of change of θ along the z-axis. Deriving from the theory of surfaces, a helicoil (Fig. 3) has infinite radius of curvature with respect to the coordinates (r, θ), whereas the radius of twist (or torsion of the space curve r) is finite [11, 12] as shown in Figures 5 and 6, *i.e.*,

$$\frac{1}{R_r} = 0; \quad \frac{1}{R_\theta} = 0; \quad \frac{1}{R_{r\theta}} = -\frac{\varphi}{1 + r^2\varphi^2} \qquad \text{(2a, b, c)}$$

where R_r and R_θ are the radius of curvatures in the r- and θ-directions, respectively, and $R_{r\theta}$ is the radius of twist.

In Figure 5, large nonlinear twisting curvature versus r/a, for constant θ_0, is presented. Considering a specific length a (Fig. 2), the twisting curvature at a point r from the axis would be almost linear to the distance r if the projected angle θ_0 is small ($\theta_0 \leq 30°$). For larger θ_0, the nonlinearity effect becomes more obvious, and the twisting curvature decreases dramatically for a point moving from the axis outwards radially (along the r-direction). In Figure 6, the relationship of twisting curvature with respect to varying θ_0, for constant r/a, is presented. Considering a specific length a, the twisting curvature at a point r from the axis increases first, when the projected angle θ_0 increases. However, as θ_0 further increases, the twisting curvature reaches a maximum before it starts decreasing. Therefore, in order to achieve maximum twisting curvature, θ_0 should maintain a particular relationship with respect to r/a, as shown in Figure 6. For instance, for a constant $r = r_1$, we may differentiate Eq. (2c) with respect to φ and

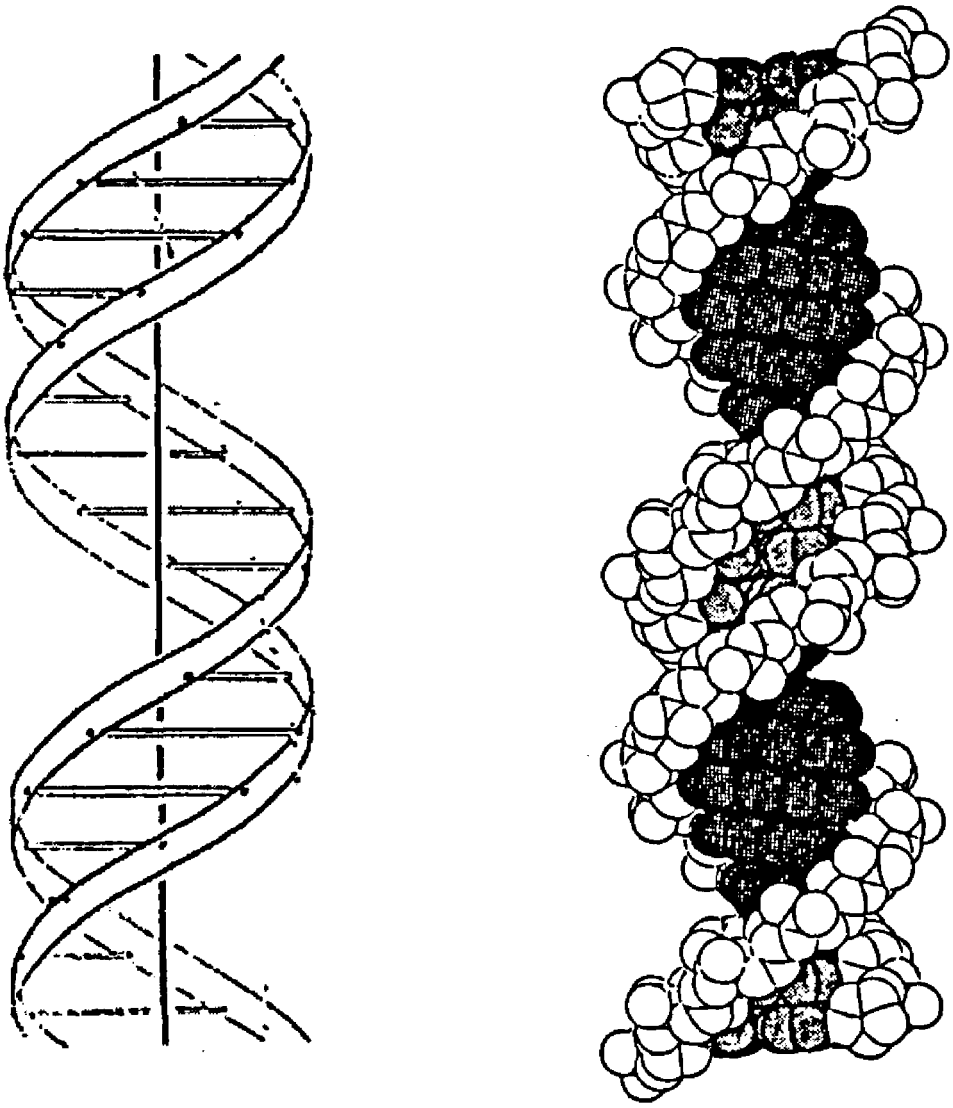

FIGURE 4 (a) A double helicoidal DNA model with bonding and (b) A DNA molecule.

set it to zero, $\mathrm{d}|1/R_{r\theta}|/\mathrm{d}\varphi = 0$. We then determine that for maximum $|1/R_{r\theta}|$, $\varphi = 1/r_1$ and $|1/R_{r\theta}|_{\max} = \varphi/2$.

The derivation of nonlinear twisting curvature (2c) [11, 12] is a benchmark, as it has generalized the conventional linear twisting curvature $1/R_{r\theta} \approx -\tan\varphi$ for a small φ [7, 9, 10]. Thus, it is possible to analyze a highly twisted helicoidal structure. There exist two inherent approximations in assuming $1/R_{r\theta} \approx -\tan\varphi$, the first being $\varphi \approx \tan\varphi$ and the second $r\varphi \ll 1$. For the first assumption, an approximately 10% error will occur for $\theta_0 = 30°$; for the second assumption, $\theta_0(r/a) = 0.26 \ll 1$ for $r/a = 0.5$ is very unsatisfactory.

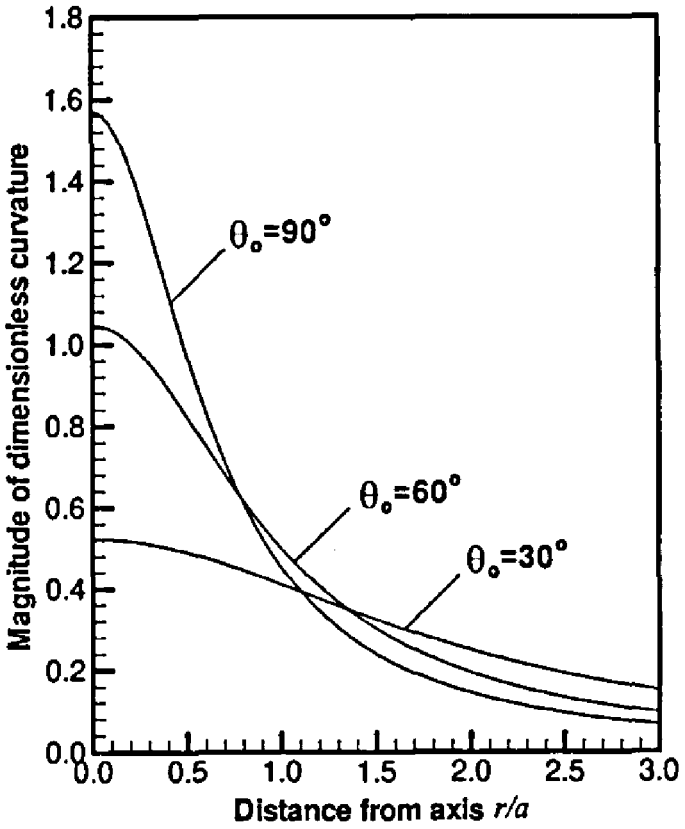

FIGURE 5 Large nonlinear twisting curvature for constant θ_0.

Let $\bar{\mathbf{u}}(t, r, \theta)$ be the time-dependent, t, displacement vector composing of u_r, u_θ in the osculating plane and u_b in the binormal direction, the linear normal and shear strains [11, 12] are:

$$\varepsilon_{rr} = \frac{\partial u_r}{\partial r}; \quad \varepsilon_{\theta\theta} = \frac{1}{h_\theta}\frac{\partial u_\theta}{\partial \theta} + \frac{r u_r}{h_\theta^2}; \quad \gamma_{r\theta} = \frac{\partial u_\theta}{\partial r} - \frac{r u_\theta}{h_\theta^2} + \frac{1}{h_\theta}\frac{\partial u_r}{\partial \theta} - \frac{2u_b}{\varphi h_\theta^2} \tag{3a, b, c}$$

$$\kappa_{rr} = -\frac{3}{2\varphi h_\theta^2}\frac{\partial u_\theta}{\partial r} + \frac{3 r u_\theta}{2\varphi h_\theta^4} - \frac{\partial^2 u_b}{\partial r^2} + \frac{1}{2\varphi h_\theta^3}\frac{\partial u_r}{\partial \theta} \tag{3d}$$

$$\kappa_{\theta\theta} = -\frac{3}{2\varphi h_\theta^3}\frac{\partial u_r}{\partial \theta} - \frac{1}{h_\theta^2}\frac{\partial^2 u_b}{\partial \theta^2} - \frac{r u_\theta}{2\varphi h_\theta^4} - \frac{r}{h_\theta^2}\frac{\partial u_b}{\partial r} + \frac{1}{2\varphi h_\theta^2}\frac{\partial u_\theta}{\partial r} \tag{3e}$$

$$\tau_{r\theta} = \frac{1}{h_\theta}\frac{\partial^2 u_b}{\partial r \partial \theta} + \frac{r}{h_\theta^3}\frac{\partial u_b}{\partial \theta} - \frac{1}{\varphi h_\theta^2}\frac{\partial u_r}{\partial r} - \frac{1}{\varphi h_\theta^3}\frac{\partial u_\theta}{\partial \theta} + \frac{r u_r}{\varphi h_\theta^4} \tag{3f}$$

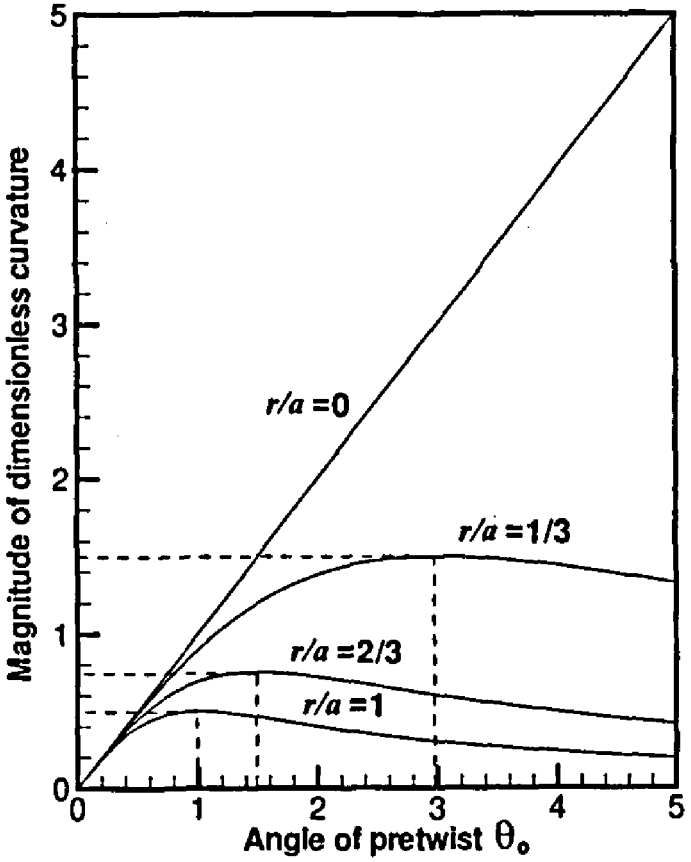

FIGURE 6 Large nonlinear twisting curvature for constant r/a.

where $h_\theta = (1/\varphi)\sqrt{1 + r^2\varphi^2}$ is the metric tensor of the helicoidal coordinate system. During deformation, the stretching strain energy and bending strain energy for constant thickness h can be expressed as

$$U = \frac{6D}{h^2}\int\int_A \left[\varepsilon_{rr}^2 + \varepsilon_{\theta\theta}^2 + 2\nu\varepsilon_{rr}\varepsilon_{\theta\theta} + \frac{1-\nu}{2}\gamma_{r\theta}^2\right] h_\theta \, dr \, d\theta$$
$$+ \frac{D}{2}\int\int_A [\kappa_{rr}^2 + \kappa_{\theta\theta}^2 + 2\nu\kappa_{rr}\kappa_{\theta\theta} + 2(1-\nu)\tau_{r\theta}^2] h_\theta \, dr \, d\theta, \qquad (4)$$

corresponding to the first and second integrals, respectively, where $D = Eh^3/12(1-\nu^2)$ is the flexural rigidity with E and ν representing the Young's modulus and Poison's ratio. Equations for varying thickness $h(r, \theta)$ can be reformulated accordingly, by moving $h^3(r, \theta)$ present in D into the domain integrals for strain (first domain integral in Eq. (4)) and change of curvature (second domain integral in Eq. (4)).

The work done due to fluid excitation is

$$W = \int\int_A \vec{\mathbf{q}}(t, r, \theta) \cdot \vec{\mathbf{u}}(t, r, \theta) h_\theta \, dr \, d\theta \tag{5}$$

where $\vec{\mathbf{q}}(t, r, \theta)$ is the time-dependent fluid loading distribution over domain A. Assuming admissible displacement functions for u_r, u_θ, u_b, defining an energy functional as

$$F = U - W, \tag{6}$$

and minimizing F in accordance with the variational principle result in a system of homogeneous equations as

$$[\mathbf{K}]\{\mathbf{C}\} - \{\mathbf{Q}\} = 0 \tag{7}$$

where [K], {C}, {Q} are the stiffness matrix, displacement coefficient and external loadings. Solving this system of homogeneous equations gives the response of the Watson–Crick DNA model subject to external fluid excitations.

For nonlinear large deformation analysis, some linear relations such as the strain-displacement relationships (3a–f) and strain energy (4) must be reformulated. A number of nonlinear terms comprising $(\partial u_b/\partial r)^2$, $(\partial u_b/\partial \theta)^2$ *etc.* will be involved. Combining with the fluid flow excitations, the governing equation may have to be solved repeatedly and recursively. Some root-finding numerical procedures such as Powell's hybrid algorithm, an improved variation of Newton's method, may be employed.

If thickness-to-width ratio h/b is of the order $O(10^{-1})$ or lower, first-order or higher-order displacement functions, depending on the thickness coordinate, must be adopted [17]. A three-dimensional elasticity model [18] on *one unit* (360°) of the repeating helicoil may also be solved for more accurate solutions. All formulation and equations derived for a modeling in Figure 2 are valid for a helicoil model in Figure 3.

3 LOW-REYNOLDS-NUMBER FLUID EXCITATION

The organic fluid in the nucleus of a living cell, in which DNA is submerged, is highly viscous and undergoes low speed motion. Precisely, it has a low Reynolds number defined as

$$R_e = \frac{\rho U L}{\mu} \tag{8}$$

where ρ, U, μ are respectively the fluid density, speed, dynamic viscosity and L is a typical dimension. In investigating flows at low Reynolds numbers, it is customary to linearize the Navier–Stokes equations, in order to obviate a prohibitively difficult problem of obtaining complete, analytical solutions. A useful method for solving such linearized flows is the singularity method, where the solution is expressed in terms of discrete or continuous distributions of fundamental singularities [15]. For steady viscous flows, a set of new fundamental solutions called Stokesons, rotons and stressons was first introduced [15]. This approach has recently been further extended to unsteady, time-dependent Stokes flows and general fundamental solutions in an arbitrary temporal domain were presented [16]. For the analysis of DNA dynamics, the organic fluid flow is governed by [16]:

$$\nabla \cdot \vec{\mathbf{v}} = 0 \tag{9}$$

$$\frac{\partial \vec{\mathbf{v}}}{\partial t} + \vec{\mathbf{V}} \cdot \nabla \vec{\mathbf{v}} - \nabla \times [(\vec{\Omega} \times \vec{\mathbf{x}}) \times \vec{\mathbf{v}}] = -\nabla p + \nabla^2 \vec{\mathbf{v}} + \vec{\mathbf{q}}(t, \mathbf{x}) \tag{10}$$

where $\vec{\mathbf{V}}$, $\vec{\Omega}$ are the flow velocity and angular velocity; $\vec{\mathbf{v}}, p$ are the disturbed flow velocity and pressure, $\vec{\mathbf{q}}(t, \vec{\mathbf{x}})$ is the time-dependent fluid force distribution in the flow field $\vec{\mathbf{x}}$, related to the quantity in Eq. (5). A fundamental solution for the unsteady Oseen flow is [16]

$$\|\vec{\mathbf{q}}\| = \frac{8\pi}{1 + 2K_0(t/4; R_e/4)} \tag{11a}$$

where

$$K_n(t; \alpha) = \frac{1}{2}\left(\frac{\alpha}{2}\right)^n \int_0^t \frac{e^{-\beta - (\alpha^2/4\beta)}}{\beta^{n+1}}\, d\beta \tag{11b}$$

Decomposing $\vec{\mathbf{q}}$ into q_r, q_0, q_b and substituting them into Eq. (5), the work done by the fluid loading on the helicoidal structure can be determined.

4 NUMERICAL EXAMPLES

Consider a single, infinitely long helicoil, as shown Figure 3, immersed in a viscous flow field having a constant, steady fluid loading $\vec{\mathbf{q}} = q\vec{\mathbf{i}}$ in the positive x-direction. As the helicoil is assumed infinitely long, it is possible to analyze only *one unit* (360°) of the repeating helicoil. From Eq. (1) and Figure 1, the unit normal vectors in the orthogonal coordinate system $(\vec{\mathbf{r}}, \partial\vec{\mathbf{r}}/\partial\theta, \vec{\mathbf{b}})$ can be found as

$$\begin{aligned}
\vec{\mathbf{e}}_r &= \cos\theta\,\vec{\mathbf{i}} + \sin\theta\,\vec{\mathbf{j}} \\
\vec{\mathbf{e}}_\theta &= \frac{\varphi}{\sqrt{1+r^2\varphi^2}}\left[-r\sin\theta\,\vec{\mathbf{i}} + r\cos\theta\,\vec{\mathbf{j}} + \frac{1}{\varphi}\vec{\mathbf{k}}\right] \\
\vec{\mathbf{e}}_b &= \frac{1}{\sqrt{1+r^2\varphi^2}}[\sin\theta\,\vec{\mathbf{i}} - \cos\theta\,\vec{\mathbf{j}} + r\varphi\vec{\mathbf{k}}]
\end{aligned} \tag{12}$$

Decomposing $\vec{\mathbf{q}} = q\vec{\mathbf{i}}$ in the orthogonal coordinate system $(\vec{\mathbf{r}}, \partial\vec{\mathbf{r}}/\partial\theta, \vec{\mathbf{b}})$ provides

$$\vec{\mathbf{q}} = q\cos\theta\vec{\mathbf{e}}_r - \frac{qr\varphi\sin\theta}{\sqrt{1+r^2\varphi^2}}\vec{\mathbf{e}}_\theta + \frac{q\sin\theta}{\sqrt{1+r^2\varphi^2}}\vec{\mathbf{e}}_b \tag{13}$$

Substituting the flow loading in Eq. (13) into Eq. (5) yields the work done by flow on the helicoil as

$$W = q\int\int_A \left[h_\theta\cos\theta\,u_r - r\sin\theta\,u_\theta + \frac{\sin\theta}{\varphi}u_b\right]\mathrm{d}r\,\mathrm{d}\theta \tag{14}$$

The displacement field (u_r, u_θ, u_b) may be represented as an infinite polynomial series as

$$\begin{aligned}
u_r &= \sum_{i=1}^{m} C_i^r \phi_i^r(x,y) \\
u_\theta &= \sum_{i=1}^{m} C_i^\theta \phi_i^\theta(x,y) \\
u_b &= \sum_{i=1}^{m} C_i^b \phi_i^b(x,y)
\end{aligned} \tag{15}$$

where C_i^r, C_i^θ, C_i^b are unknown coefficients and ϕ_i^r, ϕ_i^θ, ϕ_i^b are truncated, complete two-dimensional polynomial series.

Due to geometric symmetry of a helicoil for every cycle of 360° along the axis, we may impose the following boundary conditions when analyzing one cycle of helicoil. At the two boundaries when $\theta = 0°$ and $\theta = 360°$,

$$u_\theta = u_b = 0 \tag{16}$$

while $u_r \neq 0$ because the helicoil is subjected to a flow loading in the r-direction. These boundary conditions can be imposed to the strain energy and work expressions in Eqs. (4) and (14), respectively.

Substituting strain energy and work done into the energy functional in Eq. (6) and minimizing in accordance with the variational principle with respect to the unknown coefficients

$$\frac{\partial F}{\partial C_i^r} = \frac{\partial F}{\partial C_i^\theta} = \frac{\partial F}{\partial C_i^b} = 0 \tag{17}$$

result in a system of homogeneous equations as given by Eq. (7). This system can be solved numerically using a standard numerical solver, such as the IMSL library in Fortran, to obtain the deformation solution.

Two numerical examples are provided in Figures 7 and 8 for infinite helicoils with width-to-radius b/R equal to 0.4 and 0.7, respectively, for a dimensionless fluid loading of $qR^3/D = 1$. On the left of the figures show the deformed mode shape of one-unit (360°) of helicoil, on the middle and right show the values of dimensionless orthogonal deformation components $\bar{u}_r = u_r/R$, $\bar{u}_\theta = u_\theta/R$, $\bar{u}_b = u_b/R$ and their resultant $\bar{u} = \sqrt{\bar{u}_r^2 + \bar{u}_\theta^2 + \bar{u}_b^2}$ for the inner (closer to the axis) and outer (further to the axis) boundaries, respectively. It is interesting to note that $\bar{u}_r$, $\bar{u}_\theta$, $\bar{u}_b$ and $\bar{u}$ are periodic with respect to one-cycle of dimensionless height or 360° of helicoil. This is expected as we analyze an infinitely long helicoil and due to symmetry in geometry and flow loading, the deformation pattern repeats itself for every cycle of dimensionless height along the axis.

It is also observed that the outer boundary deformed higher than the inner boundary. As we have discussed in Section 2 and Figures 5 and 6, the magnitude of twisting curvature varies along the radial direction of the twisting helicoil. As stiffness is dependent of the magnitude of twisting curvature, the inner and outer boundaries would have different deformation in general. For the inner and outer boundaries, $\bar{u}_r$ and $\bar{u}_b$ components deform in a similar direction while $\bar{u}_\theta$ component deforms in opposite directions.

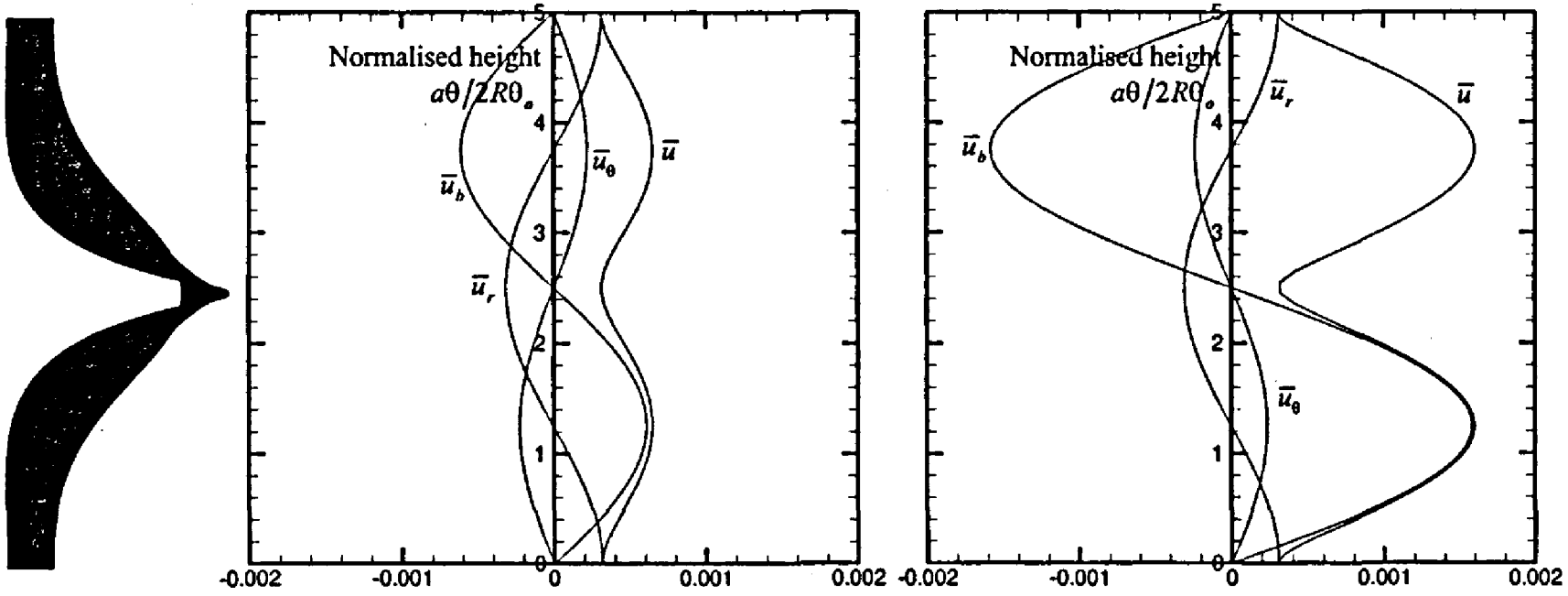

(a) Deformed mode shape (b) Deformation of inner boundary (c) Deformation of outer boundary

FIGURE 7 Deformation of an infinite helicoil with $b/R = 0.4$, $h/R = 0.02$, $a/R = 10$, $\theta_0 = 360°$ and $qR^3/D = 1$.

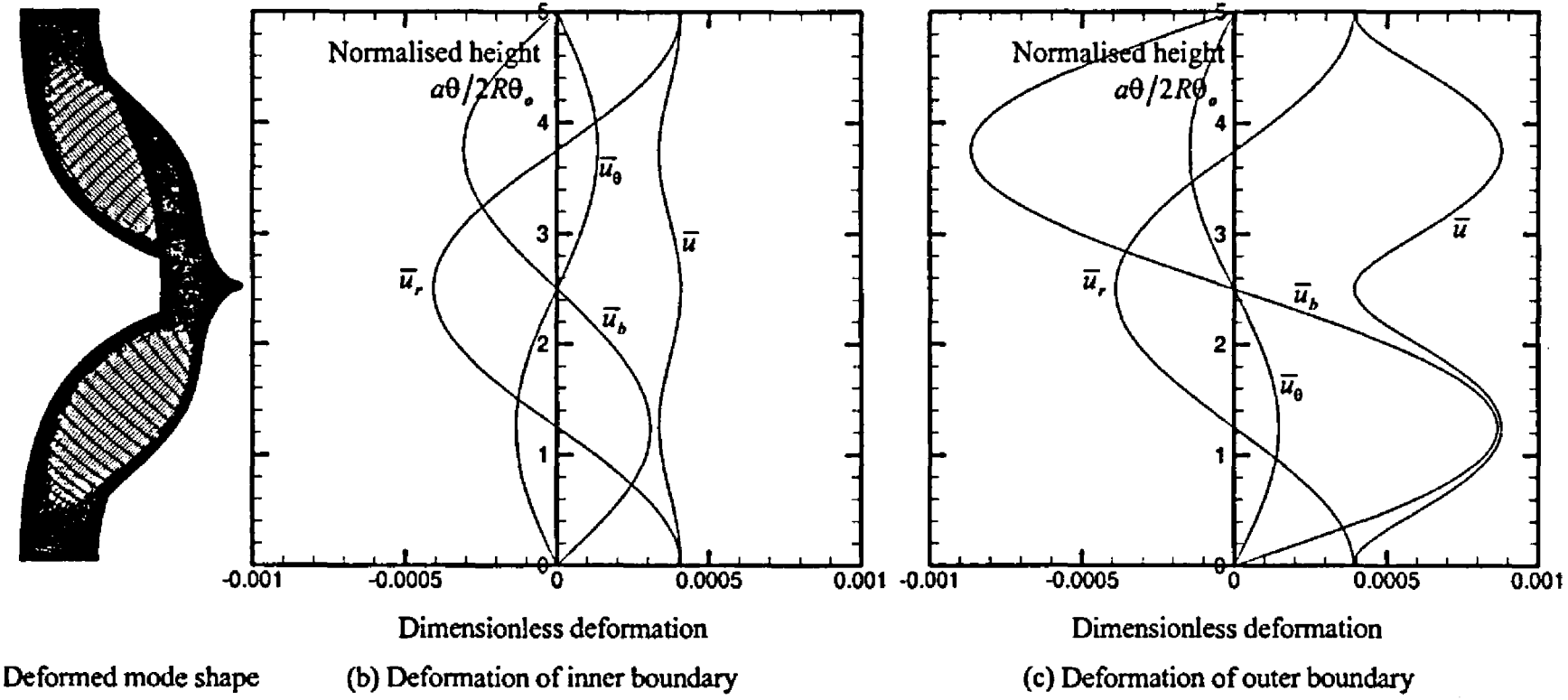

(a) Deformed mode shape (b) Deformation of inner boundary (c) Deformation of outer boundary

FIGURE 8 Deformation of an infinite helicoil with $b/R = 0.7$, $h/R = 0.02$, $a/R = 10$, $\theta_0 = 360°$ and $qR^3/D = 1$.

Comparing Figures 7 and 8, the corresponding dimensionless deformation components are of similar patterns because we assumed a linear, steady flow loading in these examples. A decrease in structural stiffness or an increase in flow loading will anticipate an increase in deformation amplitude. For instance, the overall stiffness of a narrower helicoil ($b/R = 0.4$) in Figure 7 is smaller than the overall stiffness of a wider helicoil ($b/R = 0.7$) in Figure 8. Therefore, the magnitude of deformation in Figure 7 is higher than the corresponding values in Figure 8. Therefore, by adjusting the width of the helicoil, it is possible to simulate the stiffness of a helicoidal structure and the quantity of flow loading without changing the magnitude of flow loading distribution on the helicoidal structure, which is $qR^3/D = 1$ in these examples. It is also possible to adopt a varying thickness helicoil $h(r, \theta)$ so that the stiffness at any single point on the domain of helicoil could be characterized accordingly to simulate the stiffness of a DNA double helix. Further work and examples in this area will be conducted to accommodated nonlinear flow field with nonlinear deformation of helicoils.

On knowing the structural characteristics of DNA molecules, an efficient structural model could be constructed. Further analysis of the DNA molecules could be focused on measuring the mechanical parameters, such as distributions of deformation, bending and twisting, of the deformed DNA.

CONCLUDING REMARKS

The paper is devoted to a new and rapidly developing field of life sciences, the nonlinear physics of DNA. A theoretical model for helicoidal structures subject to viscous fluid excitations at a low-Reynolds-number is presented herewith. It aims to model bio- nonlinear DNA dynamics mechanically from a fluid-structure interaction approach. Constructing a physical model for systematic and consistent analysis of the internal biomechanical structure of DNA is significant and valuable. Besides cultivating an understanding of life science, the matching of DNA sequential characteristics with respect to the dynamical responses will reveal information regarding DNA sequencing by means of its twisting and bending motions. Two numerical examples for linear, steady flows on an infinite helicoidal structure are presented to outline the idea and procedure of computation.

Acknowledgements

The work described in this paper was substantially supported by a grant from City University of Hong Kong [Project No. 7100161 (BC)]. The authors very much appreciate the constructive suggestions made by Professor Dhanjoo N. Ghista.

References

[1] Watson, J. D. and Crick, F. H. C. (1953) "Molecular structure of nucleic acids. A structure of deoxyribose nuclei acid", *Nature* **171**, 737–738.
[2] Yakushevich, L. V. (1998) *Nonlinear Physics of DNA* (John Wiley and Sons, New York).
[3] Crick, F. H. C. (1988) "An anecdotal history of the discovery of the structure of DNA and of the genetic code", *What Mad Pursuit* (Weidenfeld and Nicolson, London).
[4] Calladine, C. R. and Drew, H. R. (1997) *Understanding DNA, The Molecule and How it Works*, 2nd ed. (Academic Press, New York).
[5] Davydov, A. S. (1979) "Solitons in Molecular Systems", *Physica Scripta* **20**, 387–394.
[6] Englander, S. W., Kallenbach, N. R., Heeger, A. J., Krumhansl, J. A. and Litwin, A. (1980) "Nature of the open state in long polynucleotide double helices: Possibility of soliton excitations", *Proceedings of the National Academy of Sciences of the United States of America* **77**, 7222–7226.
[7] Leissa, A. W., MacBain, J. C. and Kielb, R. E. (1984) "Vibrations of twisted cantilevered plates–Summary of previous and current studies", *Journal of Sound and Vibration* **96**, 159–173.
[8] Leung, A. Y. T. (1991) "Exact stiffness matrix for twisted helix beam", *Finite Elements in Analysis and Design* **9**, 23–32.
[9] Lim, C. W. and Liew, K. M. (1995) "Vibration of pretwisted cantilever trapezoidal symmetric laminates", *Acta Mechanica* **111**, 193–208.
[10] Lim, C. W., Liew, K. M. and Kitipornchai, S. (1997) "Free vibration of pretwisted cantilevered composite shallow conical shells", *AIAA Journal* **35**(2), 327–333.
[11] Lim, C. W. (1999) "An exact helicoidal model for vibration of turbomachinery blades", Proceedings of ASME Mechanical and Material Conference, USA, p. 441.
[12] Lim, C. W. (1999) "Investigating the limit of turbomachinery blade modelling with linear pretwist", Proceedings of the 2nd International Symposium on Vibration and Continuous System, Switzerland, pp. 33–35.
[13] Barkley, M. D. and Zimm, B. H. (1979) "Theory of twisting and bending of chain macromolecules; analysis of the fluorescence depolarization of DNA", *The Journal of Chemical Physics* **70**, 2991–3007.
[14] Allison, A. and Shurr, J. M. (1979) "Torsion dynamics and depolarization of fluorescence of linear macromolecules. 1. Theory and application to DNA", *Chemical Physics* **41**, 35–59.
[15] Chwang, A. T. and Wu, T.Y.-T. (1975) "Hydromechanics of low-Reynolds-number flow. Part 2. Singularity method for Stokes flows", *Journal of Fluid Mechanics* **67**, 787–815.
[16] Shu, J.-J. and Chwang, A. T. (2001) "Generalized fundamental solutions for unsteady viscous flows", *Physical Review E* **63**(5), 051201.
[17] Lim, C. W. and Liew, K. M. (1995) "A higher order theory for vibration of shear deformable cylindrical shallow shells", *International Journal of Mechanical Sciences* **37**(3), 277–295.
[18] Lim, C. W. (1999) "Three dimensional vibration analysis of a cantilevered parallelepiped: Exact and approximate solutions", *Journal of the Acoustical Society of America* **106**(6), 3375–3383.